

# High-resolution near-infrared speckle interferometry and radiative transfer modeling of the OH/IR star OH 104.9+2.4

D. Riechers<sup>(1,2)</sup>, T. Driebe<sup>(2)</sup>, Y. Y. Balega<sup>(3)</sup>, K.-H. Hofmann<sup>(2)</sup>,  
A. B. Men'shchikov<sup>(4),(2)</sup>, and G. Weigelt<sup>(2)</sup>

(1) Max-Planck-Institut für Astronomie, Heidelberg, Germany

(2) Max-Planck-Institut für Radioastronomie, Bonn, Germany

(3) Special Astrophysical Observatory, Nizhnij Arkhyz, Karachaevo-Cherkesia, Russia

(4) Institute for Computational Astrophysics, Saint Mary's University, Halifax, Canada



MAX-PLANCK-GESELLSCHAFT

## Abstract

We present near-infrared speckle interferometry of the OH/IR star OH 104.9+2.4 in the  $K'$  band obtained with the 6m telescope of the Special Astrophysical Observatory (SAO) in Oct. 2002 and 2003. At a wavelength of  $\lambda = 2.13 \mu\text{m}$  the diffraction-limited resolution of 74 mas was attained. The reconstructed visibility reveals a spherically symmetric, circumstellar dust shell (CDS) surrounding the central star. The visibility function shows that the stellar contribution to the total flux at  $\lambda = 2.13 \mu\text{m}$  is less than 30% at all phases, indicating a rather large optical depth of the CDS. The azimuthally averaged 1-dimensional Gaussian visibility fit yields a diameter of  $47 \pm 3 \text{ mas}$  (FWHM), which corresponds to  $112 \pm 13 \text{ AU}$  for an adopted distance of  $D = 2.38 \pm 0.24 \text{ kpc}$ . To determine the structure and the properties of the CDS of OH 104.9+2.4, radiative transfer calculations using the code DUSTY were performed to simultaneously model its visibility and the spectral energy distribution (SED). Since OH 104.9+2.4 is highly variable, the observational data taken into consideration for the modeling correspond to different phases of the object's variability cycle. This offers the possibility to derive several physical parameters of the central star and its CDS as a function of phase. For instance, according to our final model the effective temperature of the central star increases from  $T_{\text{eff}} = 2250 \text{ K}$  at minimum phase ( $\Phi = 0.5$ ) to  $T_{\text{eff}} = 3150 \text{ K}$  at maximum phase ( $\Phi = 0.0$ ), while the stellar radius decreases from  $R = 730 R_{\odot}$  at  $\Phi = 0.5$  to  $675 R_{\odot}$  at  $\Phi = 0.0$ . For the CDS, we found that the inner boundary of the dust shell is located at  $8.3 R_{\odot}$  at minimum phase and approximately a factor of two further away at maximum phase ( $R_{\text{in}}/R_{\odot} = 17.5$ ), and the optical depth at  $2.2 \mu\text{m}$  decreases from 8.5 to 3.5 between minimum and maximum phase. Our detailed analysis demonstrates the potential of dust shell modeling constrained by both the SED and visibilities obtained from interferometric measurements.

## Introduction

OH/IR stars are long-period variables (LPVs, pulsation periods between 500 and 3000 d) of variability type Me, similar to long-period Mira stars. While the majority of these stars show a bolometric amplitude of typically  $\sim 1^{\text{m}}$  a very small fraction varies irregularly with a low amplitude or does not show any detectable variability. OH/IR stars are mostly low and intermediate mass (progenitor masses  $M \leq 9 M_{\odot}$ ), oxygen-rich single stars evolving along the upper part of the asymptotic giant branch (AGB). Thus, they stars extend the sequence of optical Mira variables towards longer periods, larger optical depths and higher mass-loss rates. As a consequence of their high mass loss, OH/IR stars are surrounded by massive, optically and geometrically thick circumstellar envelopes composed of gas and dust. OH 104.9+2.4 is an OH/IR type II-A class star. These objects exhibit the maximum of their SED in the infrared (IR) around 6-10  $\mu\text{m}$ , while the 9.7  $\mu\text{m}$  silicate feature is found in absorption due to the presence of an optically thick circumstellar envelope. OH 104.9+2.4 is  $D = 2.38 \pm 0.24 \text{ kpc}$  away (distance obtained with the MASER phase lag method, see [1]), and the central AGB star is a long-period variable with  $P \approx 1500 \text{ d}$ .

## Observations

We obtained visibilities from speckle-interferometric observations with the SAO 6m telescope on Sep 22, 2002 and Oct 11, 2003 by applying the speckle interferometry method [2]. The measurements were accomplished with a  $K'$ -band filter at  $\lambda = 2.13 \mu\text{m}$  ( $FWHM = 0.11 \mu\text{m}$ ). Although obtained at different epochs, both visibilities exhibit striking similarity and reveal that the CDS is fully resolved by our measurements (see Fig. 1). From the 2D-visibilities no major deviation of the CDS from spherical symmetry could be detected.

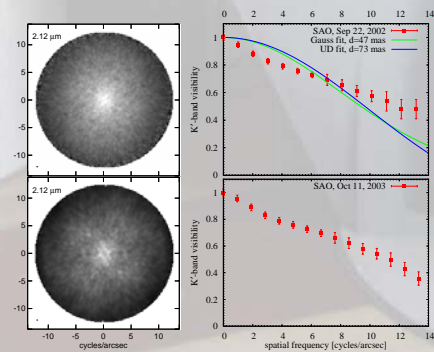
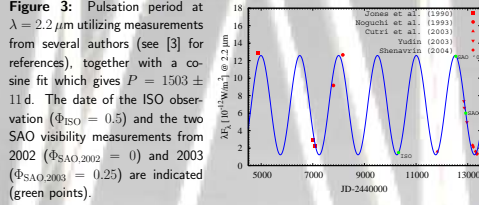


**Figure 2:** SAO Observations of OH 104.9+2.4 on Sep 22, 2002 (upper panels) and on Oct 11, 2003 (lower panels). **Left:** 2-D  $K'$ -band visibility. **Right:** Azimuthally averaged  $K'$ -band visibility. For illustration, the visibility from 2002 is fitted with a Gaussian center-to-limb variation (CLV) [ $d_{\text{Gauss}} = 47 \pm 3 \text{ mas}$ , blue] and a uniform-disc (UD) [ $d_{\text{UD}} = 73 \pm 5 \text{ mas}$ , green] model as a first, rough estimate for the diameter of the CDS.



Since we used the bolometric flux as input for our radiative transfer calculations of the variable object OH 104.9+2.4, we first had to determine the phases of the visibility and ISO measurements and the values of  $F_{\text{bol}}$  at these phases. Using new  $K'$ -band photometric measurements and data available from the literature (see [3] for references) we fitted a cosine function to determine the pulsation period of OH 104.9+2.4 and the variability phases corresponding to the epochs of the visibility and ISO measurements. We derived a period  $P = 1500 \pm 11 \text{ d}$  and phases  $\Phi_{\text{ISO}} = 0.5$ ,  $\Phi_{\text{SAO,2002}} = 0.0$ , and  $\Phi_{\text{SAO,2003}} = 0.25$  (see Fig. 3). For the bolometric flux derived from the 1996 ISO SED data we found  $F_{\text{bol,ISO}} = F_{\text{bol,min}} = 0.7 \cdot 10^{-10} \text{ W/m}^2$ , and from available photometry close to  $\Phi = 0.0$  (see [3] for references) we estimated  $F_{\text{bol,SAO,2002}} = F_{\text{bol,max}} = 2.3 \cdot 10^{-10} \text{ W/m}^2$ , i.e. the bolometric flux changes by a factor of  $\sim 3.3$  between maximum and minimum phase.

## Radiative Transfer Modeling

Our goal was to simultaneously model the  $K'$ -band visibilities and the SED of OH 104.9+2.4 measured at different epochs to determine the temporal change of some physical parameters of the CDS. To accomplish this goal, we used the 1-D radiative transfer code DUSTY [4,5] to scan large fractions of the corresponding parameter space. Several  $10^5$  models were calculated. DUSTY utilizes the IR signature of the dusty medium to analyze the structure of the optically obscured object. The input parameters of the code are the spectral shape  $f_{\nu} = F_{\nu}/F_{\text{bol}}$  of the central source, general dust absorption properties and scattering cross sections (dust chemistry), the dust density profile, an optical depth  $\tau_{\nu}$  at a reference wavelength  $\mu$ , and the temperature at the inner dust shell boundary. In our calculations, we used a  $n(a) \propto a^{-3.5}$  grain-size distribution ([6]). We found that the observations can be best reproduced using the cold silicates from Suh ([7]) and a density distribution which is calculated from a radiatively driven wind approach ([4,5]). As the DUSTY code does not correct for interstellar reddening, we added a routine to redden the models assuming  $A_V = 3.3$ .

The model parameters of our quasi-time-dependent model are summarized in Tab. 1. As the table shows, due to its variability the temperature of the central source increases by  $\sim 900 \text{ K}$  from minimum to maximum phase while the stellar radius decreases by  $\sim 55 R_{\odot}$  ( $= 8\%$ ). Correspondingly, the inner dust shell boundary moves from  $8.3$  to  $17.5 R_{\odot}$ , and the optical depth in the  $10 \mu\text{m}$  regime drops by a factor  $\sim 2.4$ .

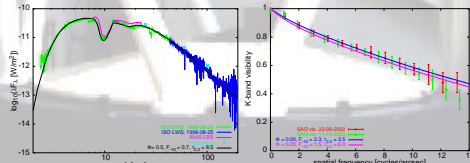


**Figure 4:** Comparison of SED (left) and  $K'$  visibility (right) from our best-fitting model with the ISO and SAO measurements of OH 104.9+2.4. Note that different bolometric flux values have been used for the SED and visibility model in order to account for the different epochs/phases of the observations. See Tab. 1 for a summary of our model parameters.

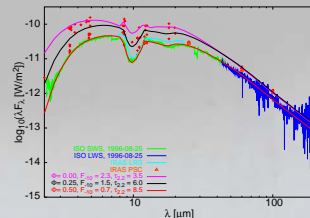


**Figure 5:** Variation of the SED with the pulsation phase of the central LPV. The model SED is shown for three different phases ( $\Phi = 0.0, 0.25, \text{ and } 0.5$ ). In addition, ISO and IRAS spectra as well as various photometric measurements are displayed (see [3] and [8] for references on the measurements indicated by red crosses). As the figure shows, all measurements are fully bracketed by the model SEDs for minimum and maximum phase.

Parameter	$\Phi = 0.5$ (1996)	$\Phi = 0$ (2002)	$\Phi = 0.25$ (2003)
Effective temperature $T_{\text{eff}}$ [K]	2250	3150	2800
Temperature at inner $T_{\text{in}}$ [K]	1000		
CDS boundary*			
Relative CDS thickness* $r_{\text{out}}/r_{\text{in}}$	$10^5$		
Minimum grain size* $a_{\text{min}}$ [ $\mu\text{m}$ ]	0.005		
Maximum grain size* $a_{\text{max}}$ [ $\mu\text{m}$ ]	0.28		
Dust-to-gas ratio* $r_{\text{dg}}$	0.005		
Dust grain bulk density* $r_s$ [ $\text{g cm}^{-3}$ ]	3.0		
Optical depth			
$\tau_{0.75 \mu\text{m}}$	146.7	60.4	103.6
$\tau_{2.2 \mu\text{m}}$	8.5	3.5	6.0
$\tau_{9.7 \mu\text{m}}$	13.9	5.7	9.8
Central star radius $R_*$ [ $R_{\odot}$ ]	729	675	691
[AU]	3.39	3.14	3.21
[mas]	1.43	1.32	1.35
Inner CDS boundary $R_{\text{in}}$ [ $R_{\odot}$ ]	8.3	17.5	13.7
[AU]	28.3	55.0	44.0
[mas]	11.9	23.1	18.6
Mass-loss rate $\dot{M}$ [ $10^{-5} M_{\odot}/\text{yr}$ ]	3.09	5.69	5.17
Bolometric flux $F_{\text{bol}}$ [ $10^{-10} \text{ W/m}^2$ ]	0.7	2.3	1.5
Luminosity $L$ [ $10^4 L_{\odot}$ ]	1.23	4.03	2.63

**Table 1:** Derived and adopted physical parameters of OH 104.9+2.4 as provided by our model. Parameters that were treated as not time-dependent are indicated with \*. A distance of  $D = 2.38 \pm 0.24 \text{ kpc}$  (see [1]) and an outflow velocity of  $v_{\infty} = 15 \text{ km s}^{-1}$  (see [9]) were assumed.

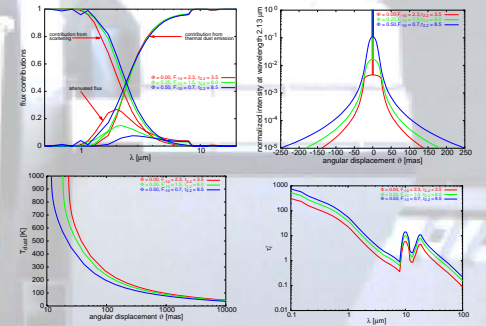


**Figure 6:** Modeling results of OH 104.9+2.4 for our best-fitting model at the pulsation phases of the ISO and SAO observations (see Tab. 1).

**Top left:** Fractional contributions to the total flux. The contribution from direct stellar light is small compared to the contribution of dust scattering and thermal emission. **Top right:** The normalized intensity profile at  $2.13 \mu\text{m}$ . The sharp central peak corresponds to the central source of radiation. **Bottom left:** Dust temperature as a function of angular distance. The point where  $T_{\text{dust}} = 1000 \text{ K}$  indicates the inner radius of the dust shell. As the figure shows, due to the variability of the central source, the inner dust shell boundary moves from  $11.9 \text{ mas}$  ( $= 8.3 R_{\odot}$ ) to  $23.1 \text{ mas}$  ( $= 17.5 R_{\odot}$ ) between minimum and maximum pulsation phase. **Bottom right:** Wavelength dependence of the total optical depth.

## Conclusions

- OH 104.9+2.4 was measured in the  $K'$  band with a diffraction-limited resolution of 74 mas at the Russian SAO 6m telescope in 2002 and 2003 using the speckle interferometry technique with very high precision. The optically thick CDS was fully resolved and no deviation from spherical symmetry was detected.
- The visibilities and the SED were simultaneously modeled with the radiative transfer code DUSTY, taking into account the variability of the source and the different epochs of the observations (quasi-time-dependent approach).
- A more detailed discussion on the modeling presented here is given in [3] and [8].

## References

- [1] Herman, J., Habing, H.J. 1985, *Astr. Astrophys. Suppl.* **59**, 523
- [2] Labeyrie, A. 1970, *A&A* **6**, 85
- [3] Riechers, D., Balega, Y.Y., Driebe, T., et al. 2004, *A&A* **424**, 165
- [4] Ivezić, Z., Elitzur, M. 1995, *ApJ* **445**, 415
- [5] Ivezić, Z., Nenkova, M., Elitzur, M. 1999, *Internal Report, Univ. of Kentucky*
- [6] Mathis, J. S., Rumpel, W., Nordiscek, K.H. 1977, *ApJ* **217**, 425
- [7] Suh, K.-W. 1999, *MNRAS* **304**, 389
- [8] Riechers, D., Balega, Y.Y., Driebe, T., et al. 2005, *A&A*, accepted
- [9] te Lintel Heckert, P., Caswell, J.L., Habing, H.J., et al. 1991, *Astr. Astrophys. Suppl.* **90**, 327

Poster presented at the ESO workshop  
The power of optical/IR interferometry: recent scientific results and 2nd generation VLTI instrumentation  
4th-8th April 2005, Garching, Germany  
contact e-mail: riechers@mpa.de, driebe@mpif-bonn.mpg.de